

True charge-transfer gap in parent insulating cuprates

A. S. Moskvina

Ural State University, 620083 Ekaterinburg, Russia

(Received 22 March 2011; revised manuscript received 16 May 2011; published 8 August 2011)

A large body of experimental data points toward a charge-transfer (CT) instability of parent insulating cuprates to be their unique property. It is argued that the true CT gap in these compounds is as small as 0.4–0.5 eV rather than 1.5–2.0 eV as usually derived from the optical gap measurements. In fact we deal with a competition of the conventional ($3d^9$) ground state and a CT state with the formation of electron-hole dimers which evolves under doping to an unconventional bosonic system. My conjecture does provide an unified standpoint on the main experimental findings for parent cuprates including linear and nonlinear optical, Raman, photoemission, photoabsorption, and transport properties related with the CT excitations. In addition I suggest a scenario for the evolution of the CuO_2 planes in the CT unstable cuprates under nonisovalent doping.

DOI: [10.1103/PhysRevB.84.075116](https://doi.org/10.1103/PhysRevB.84.075116)

PACS number(s): 71.35.-y, 74.72.Cj, 74.25.Gz

I. INTRODUCTION

The origin of high- T_c superconductivity,¹ (HTSC) is currently still a matter of great controversy. Copper oxides start out life as insulators in contrast with BCS superconductors, being conventional metals. The unconventional behavior of cuprates under charge doping, in particular, a remarkable interplay of charge, lattice, orbital, and spin degrees of freedom, strongly differs from that of ordinary metals and merely resembles that of a doped semiconductor.

I believe that the unconventional behavior of cuprates can be consistently explained in the framework of a so-called dielectric scenario² that implies their instability regarding the $d-d$ charge-transfer (CT) fluctuations. The essential physics of the doped cuprates, as well as of many other strongly correlated oxides, appears to be driven by a self-trapping of the CT excitons, both one-, and two-center ones. Such excitons are the result of self-consistent CT and lattice distortion with the appearance of a “negative- U ” effect.³

At present, the CT instability with regard to disproportionation is believed to be a rather typical property for a number of perovskite $3d$ oxides such as CaFeO_3 , SrFeO_3 , LaCuO_3 , RNiO_3 ,⁴ RMnO_3 ,⁵ and $\text{LaMn}_7\text{O}_{12}$,⁶ moreover, in solid state chemistry one considers tens of disproportionated systems.⁷ Phase diagrams of disproportionated systems are rather rich and incorporate different phase states from classical, or chemical disproportionated states, to quantum states, in particular, to the unconventional Bose superfluid (BS) (superconducting) state.²

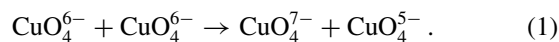
Speaking of a close relation between disproportionation and superconductivity, it is worth noting a textbook example of a BaBiO_3 system where we unexpectedly deal with the disproportionated $\text{Ba}^{3+} + \text{Ba}^{5+}$ ground state (GS) instead of the conventional lattice of Ba^{4+} cations.⁸ The bismuthate can be converted to a superconductor by a nonisovalent substitution such as in $\text{Ba}_{1-x}\text{K}_x\text{BiO}_3$. At present, this system seems to be the only one where the unconventional superconductivity is related to the disproportionation reaction.

Regrettably physicists have paid remarkably little attention to the question of valence disproportionation and negative- U approaches (“chemical” route!), which are surely are being grossly neglected in all present formal theoretical treatments of HTSC.

The paper is organized as follows. In Sec. II it is argued that the parent cuprates represent unconventional strongly correlated $3d$ oxides where strong electron-lattice polarization effects give rise to an instability with regard to a charge transfer. In Sec. III I point to the mid-infrared (MIR) absorption universally observed in all the parent two-dimensional (2D) cuprates to be a signature of the true CT gap. Section IV addresses the structure and dispersion of the CT excitons, or electron-hole (EH) dimers in parent cuprates. Section V addresses different experimental data supporting the conjecture of an anomalously small true CT gap in parent cuprates. Section VI discusses the evolution of the CT unstable parent cuprates under a nonisovalent doping.

II. ELECTRON-LATTICE RELAXATION AND CT INSTABILITY OF PARENT CUPRATES

The minimal energy cost of the optically excited disproportionation or EH formation due to a direct Franck–Condon (FC) CT transition in insulating cuprates is $E_{\text{gap}}^{\text{opt}} \approx 1.5\text{--}2$ eV. This relatively small value of the optical gap is addressed to be an argument against the “negative- U ” disproportionation reaction $2\text{Cu(II)} = \text{Cu(III)} + \text{Cu(I)}$,⁹ or, more correctly,



However, the question arises, what is the energy cost for the thermal excitation of such a local disproportionation? The answer implies, first the knowledge of relaxation energy, or the energy gain due to the lattice polarization by the localized charges. The full polarization energy R includes the cumulative effect of *electronic* and *ionic* terms, related to the displacement of electron shells and ionic cores, respectively. The former term, R_{opt} , is due to the *non-retarded* effect of the electronic polarization by the momentarily localized EH pair, given the ionic cores fixed at their perfect crystal positions. Such a situation is typical for the lattice response accompanying the FC transitions (optical excitation, photoionization). On the other hand, all the long-lived excitations, i.e., all the intrinsic thermally activated states and the extrinsic particles produced as a result of doping, injection or optical pumping should be regarded as stationary states of a system with a deformed lattice structure. A thorough

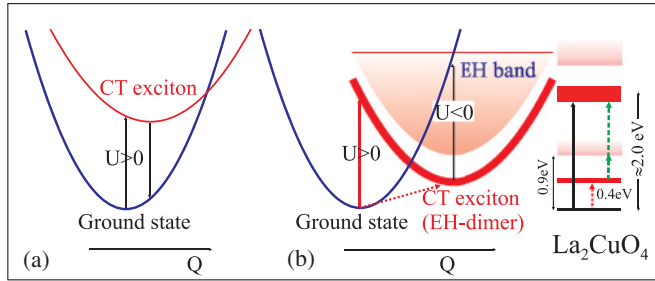


FIG. 1. (Color online) Simple illustration of the electron-lattice polarization effects for the CT excitons (see text for details): (a) CT stable system, (b) CT unstable system. The shaded area points to a continuum of unbounded electrons and holes. The right panel shows the experimentally deduced energy scheme for the CT states in La_2CuO_4 , arrows point to various CT transitions.

calculation of the localization energy for the EH pairs (EH dimers) remains a challenging task for future studies. It is worth noting that despite their very large, several electron-volt magnitudes, the relaxation effects are not incorporated into current theoretical models of cuprates.

Figure 1 illustrates two possible ways the electron-lattice polarization governs the ground state (GS) excitation evolution. Shown are the adiabatic potentials for the two-center ground state (GS) $M^0 - M^0$ configuration and excited $M^\pm - M^\mp$ CT, or disproportionated, configuration. A configurational coordinate Q is associated with a lattice degree of freedom such as a half-breathing mode. For the lower branch of adiabatic potential (AP) in the system we have either a single minimum point for the GS configuration [Fig. 1(a)] or a two-well structure with an additional local minimum point [Fig. 1(b)] associated with the self-trapped CT exciton. This “bistability” effect is of primary importance for our analysis. Indeed, these two minima are related to two (meta)stable charge states with and without CT, respectively, which form two candidates to struggle for a GS. It is worth noting that the self-trapped CT exciton may be described as a configuration with negative disproportionation energy U . Thus one concludes that all the systems such as $3d$ oxides may be separated into two classes: *CT stable systems*, with the only lower AP branch minimum for a certain charge configuration, and *bistable or CT unstable systems* with two lower AP branch minima for two local charge configurations, one of which is associated with the self-trapped CT excitons resulting from self-consistent CT and electron-lattice relaxation.

A large body of experimental findings points to an instability of the parent cuprates with regard to a CT (see, e.g., Ref. 10 and references therein). Maybe the most exciting evidence is obtained by ultrafast electron crystallography (UEC), which does provide, through observation of spatiotemporally resolved diffraction, unique tool for determining structural dynamics and the role of electron-lattice interaction.¹¹ A polarized femtosecond fs laser pulse excites the charge carriers, which relax through electron-electron and electron-phonon couplings, and the consequential structural distortion is followed diffracting fs electron pulses. The technique has revealed a structural instability in La_2CuO_4 related to the CT excitations or CT fluctuations.¹¹ Above a certain threshold, a direct conversion between two phases with distinct

electronic and structural properties of the lattice was observed, indicating that the macroscopic scale domains (which define the coherence length of the Bragg diffraction) are involved in this phase transformation. Thus the CT excitation, during its thermalization, induced distinct structural changes which distorted the lattice in a way that was observable at longer times, ≥ 300 ps.¹¹ The very slow time scale reflected the fact that electronic and structural relaxations are coupled. For the charges to fully recombine, the lattice has to relax as well, which naturally takes a long time, especially if the acoustic phonons are involved.

III. MIR BAND AS A SIGNATURE OF THE TRUE CT GAP IN PARENT CUPRATES

Unfortunately, experimental information regarding the relaxation energies for CT excitons in $3d$ oxides is scarce. Just recently, by measuring the Hall coefficient R_H up to 1000 K in La_2CuO_4 , Ono *et al.*¹² have estimated the energy gap over which the electron and hole charge carriers are thermally activated in parent cuprate La_2CuO_4 to be $\Delta_{\text{CT}} = 0.89$ eV. A true chemical potential jump between hole- and electron-doped $\text{Y}_{0.38}\text{La}_{0.62}\text{Ba}_{1.74}\text{La}_{0.26}\text{Cu}_3\text{O}_y$ (YLBLCO) was measured¹³ to be ≈ 0.8 eV. These energies may be interpreted as the minimal ones needed to create uncoupled EH pairs. Hence the minimal energy $E_{\text{gap}}^{\text{CT}}$ of the local disproportionation reaction with the creation of the relaxed bounded EH pair, or EH dimer, can be substantially less than 0.8 eV that points to a dramatic CT instability of the parent cuprate, especially, we remember that of 1.5–2.0 eV is the minimal energy of optical creation of a CT exciton or bound EH pair. This difference between the true quasiparticle gap that determines the transport and thermodynamics and the optically measured CT gap has also been found in electron-doped materials.¹⁴ In Nd_2CuO_4 the bandgap, measured as the minimum excitation energy between the hole and electron bands, is estimated to be only 0.5 eV, much lower than the optically measured CT gap, which is usually believed to be about 1.5 eV. In other words, the optical CT gap, which is generally deduced from the peak energy of the FC optical absorption, does not correspond to the true gap between the two bands in parent cuprates. However, the true CT gap $E_{\text{gap}}^{\text{CT}}$ would be optically detected as a low-energy edge of the weak non-FC (NFC) CT bands. Indeed, the dipole matrix elements for direct FC and nondirect NFC CT transitions differ mainly because of different vibrational overlap integrals, big for the former and small for the latter. Obviously, the MIR band universally found in all parent cuprates^{15–17} extending from 0.4 up to 1 eV results mainly from the weak non-FC CT optical transition whose final state corresponds to the low-energy relaxing EH dimers. In other words, the MIR band in the undoped cuprates is believed to present a non-FC counterpart of the main low-energy FC CT band. The whole line shape of the NFC+FC CT band, shown in Fig. 2 for $\text{Sr}_2\text{CuO}_2\text{Cl}_2$,^{16,18,19} is typical for other parent cuprates and would strongly deviate from that which is typical for the CT stable system. In particular, in La_2NiO_4 , which is isostructural to La_2CuO_4 , no such bands are observed¹⁵ and the line shape of the MIR absorption band in this antiferromagnet is perfectly consistent with the predictions of the pure-spin model.²⁰

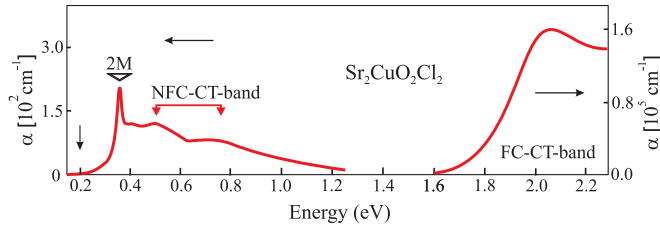


FIG. 2. (Color online) Reconstruction of the whole NFC-FC CT band in $\text{Sr}_2\text{CuO}_2\text{Cl}_2$. The low-energy MIR band is reproduced from Ref. 16, the main FC CT band is taken from Ref. 18. The scale of the respective absorption coefficients differs by three orders of magnitude. Such an unconventional NFC-FC structure of the optical spectra is a typical one for all parent cuprates. Vertical arrow points to a hardly visible peak at ≈ 0.2 eV.¹⁹

Making use of experimental data^{15–17} it is concluded that the true CT gap $E_{\text{gap}}^{\text{CT}}$ for parent cuprates such as La_2CuO_4 , Nd_2CuO_4 , Pr_2CuO_4 , $\text{Sr}_2\text{CuO}_2\text{Cl}_2$, and $\text{YBa}_2\text{Cu}_3\text{O}_6$ is as small as 0.4–0.5 eV. This puzzling result points to a remarkable CT instability of parent cuprates. It also means that the charge fluctuation in high- T_c materials are much stronger than usually believed and should be fully considered in the construction of the basic model of HTSC. It is worth noting that the d - d CT energy defines an effective U_d parameter; hence its value in parent cuprates can be as small as 0.4 eV.

It should be noted that the MIR band in parent cuprates is composed of a sharp lowest energy resonance peak and a clearly resolved two-peak high-energy structure¹⁵ with peaks near 0.4–0.5 eV and 0.7–0.8 eV, respectively (see Fig. 2). As for its FC counterpart,^{21,22} we can relate these two peaks with two-center d - d ($b_{1g} \rightarrow b_{1g}$) and one-center p - d allowed electro-dipole $b_{1g} \rightarrow e_u(\pi)$ NFC CT transitions, respectively. The EH pair related to the latter transition is composed of the $b_{1g} \propto d_{x^2-y^2}$ electron and pure oxygen $e_u(\pi)$ hole. It is worth noting that the low-energy multiplet of the EH dimers can incorporate the $b_{1g} - a_{2g}(\pi)$ pair composed of the b_{1g} electron and pure oxygen $a_{2g}(\pi)$ hole. However, the corresponding one-center p - d CT transition is electro-dipole forbidden; hence this NFC excitation as well as its FC counterpart²³ can be revealed only by the Raman scattering technique.

The energy of the lowest CT excitation is close to that of the two-magnon (2M) excitation obtained by flipping two spins on neighboring sites at the energy estimated in a spin-wave approximation as $E_{2M} = 2.73 J \approx 0.3$ – 0.4 eV.¹⁵ It indicates their strong coupling with the formation of a low-energy predominantly 2M excitation (main resonance peak at ≈ 0.35 eV in $\text{Sr}_2\text{CuO}_2\text{Cl}_2$, as seen in Fig. 2) and a high-energy, predominantly CT excitation. The coupling reduces the energy of the 2M excitation that results in lower values of exchange integrals calculated from the MIR peak position as compared with those found by neutron and Raman scattering^{16,17} In addition, the coupling makes the 2M excitation partly dipole allowed.

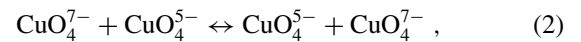
Strong coupling of the low-energy CT excitations with the high-energy magnetic excitations can explain strong deviations from the predictions of the spin-wave theory observed recently by inelastic neutron scattering in the parent cuprate La_2CuO_4 ²⁴ at high energies near the top of the spin-wave band (≈ 300 meV). While the lower energy excitations are well described by spin-wave theory, including one-magnon

and 2M scattering processes, the high-energy spin waves are strongly damped near the $(\pi, 0)$ position in reciprocal space and merge into a momentum dependent continuum. This anomalous damping indicates the decay of magnon spin waves into other excitations, possibly dispersive EH dimers.

The nature of the MIR band, unique to the layered insulating cuprates, remains one of the old mysteries of cuprate physics. To explain experimental data available for parent insulating cuprates, Lorenzana and Sawatzky²⁰ (LS) proposed the mechanism of phonon-assisted multimagnon absorption. The LS mechanism allows a successful interpretation of the experimental data on MIR absorption for $S = 1$ 2D antiferromagnet La_2NiO_4 but fails to explain all the features of the MIR in the $s = 1/2$ 2D cuprates La_2CuO_4 , Nd_2CuO_4 , $\text{Sr}_2\text{CuO}_2\text{Cl}_2$, and $\text{YBa}_2\text{Cu}_3\text{O}_6$,^{16,17,25} except the lowest-energy sharp resonance peak. The intrinsic width and the line shape of the whole MIR band remain beyond a description in terms of a spin-only Hamiltonian and point to different physics. It is worth noting that the MIR features are not susceptible to an external magnetic field. Within the error bars of the experiments, there is no systematic magnetic-field-induced changes of the MIR transmission in La_2CuO_4 in a magnetic field of 18 T.²⁶

IV. EH DIMERS IN PARENT CUPRATES

The two-center d - d CT excitons or EH dimers may be considered as quanta of disproportionation reaction (1) with the creation of electron CuO_4^{7-} and hole CuO_4^{5-} centers. The former corresponds to completely filled Cu $3d$ and O $2p$ shells, or the vacuum state for holes $|0\rangle$, while the latter may be found in different two-hole states $|2\rangle$ the first is the GS Zhang–Rice singlet.²⁷ The two EH dimers $|02\rangle$ and $|20\rangle$ will interact due to a resonance reaction $|02\rangle \leftrightarrow |20\rangle$:



governed by an effective resonance two-particle (bosonic!) transfer integral $t_{eh} = t_B$.

The energies of the two respective superposition states,

$$|\pm\rangle = \frac{1}{\sqrt{2}}(|02\rangle \pm |20\rangle),$$

are given by $E_0 \pm |t_B|$, where E_0 is the energy of the bare $|20\rangle$, $|02\rangle$ states. The even- (odd-) parity states $|\pm\rangle$ correspond to S - or P -like two-center excitons. Let us note that in our approach the S and P excitons are centered at the central oxygen ion of the Cu_2O_7 cluster shared by the both electron and hole centers.

Resonance reaction (2) corresponds to an intercenter transfer of *two holes* or *two electrons*. The magnitude of the effective resonance transfer integral t_B which determines both the excitonic even-odd or S - P splitting, and the two-particle transport is believed to be of particular interest in cuprate physics. It can be written as follows:

$$t_B = \langle 20 | V_{ee} | 02 \rangle - \sum_{11} \frac{\langle 20 | \hat{h} | 11 \rangle \langle 11 | \hat{h} | 02 \rangle}{\Delta_{dd}},$$

where the first term describes a simultaneous tunnel transfer of the electron pair due to Coulomb coupling V_{ee} and may be called a “potential” contribution, whereas the second describes

a two-step (20-11-02) electron-pair transfer via successive one-electron transfer due to a one-electron Hamiltonian \hat{h} , and may be called a “kinetic” contribution. As emphasized by Anderson,²⁸ the value of the seemingly leading kinetic contribution to pair (boson!) transport is closely related to the respective contribution to the exchange integral, i.e., $t_B \approx 0.1$ eV.

The S exciton is dipole forbidden, in contrast to the P exciton, and corresponds to a so-called two-photon state. However, these two excitons have a very strong dipole coupling with a large value of the S – P transition dipole matrix element:

$$d = |\langle S|\hat{\mathbf{d}}|P\rangle| \approx 2eR_{\text{CuCu}} \approx 8e\text{\AA}. \quad (3)$$

This points to a very important role played by this doublet in nonlinear optics, in particular in two-photon absorption and third-harmonic generation effects.^{29,30} Indeed, the quasi-1D (one-dimensional) insulating chain cuprates Sr_2CuO_3 and Ca_2CuO_3 with corner-shared CuO_4 centers show anomalously large third-order optical nonlinearities as revealed by electroreflectance,^{31,32} third-harmonic generation,³³ and two-photon absorption.^{29,34} The model fitting of the nonlinear optical features observed near 2 eV in Sr_2CuO_3 yields $E_P = 1.74$ eV, $E_S = 1.92$ eV, $\langle S|x|P\rangle = 10.5 \text{\AA}$ ³⁴ (or $\approx 8 \text{\AA}$ ³¹). Despite some discrepancies in different papers,^{31,32,34} these

parameters agree both with theoretical expectations and the data obtained in other independent measurements. In other words, the nonlinear optical measurements provide a reliable estimation of the effective “length” of the two-center d - d CT exciton and of the two-particle transfer integral: $t_B = \frac{1}{2}(E_S - E_P) \approx 0.1$ eV.

In the 2D case of an ideal CuO_2 layer we deal with two types of x -oriented (S_x, P_x) and y -oriented (S_y, P_y) S, P excitons in every unit cell whose dynamics in the framework of the Heitler–London approximation³⁵ could be described by an effective one-particle excitonic Hamiltonian with a standard form, as follows:

$$\hat{H}_{\text{exc}} = \sum_{\Gamma_1\Gamma_2\mathbf{R}_1\mathbf{R}_2} \hat{B}_{\Gamma_1}^\dagger(\mathbf{R}_1)T_{\Gamma_1\Gamma_2}(\mathbf{R}_1 - \mathbf{R}_2)\hat{B}_{\Gamma_2}(\mathbf{R}_2) \quad (4)$$

in a site representation, where $\hat{B}_{\Gamma_1}^\dagger(\mathbf{R}_1)/\hat{B}_{\Gamma_2}(\mathbf{R}_2)$ is the excitonic creation–annihilation operators, or

$$\hat{H}_{\text{exc}} = \sum_{\Gamma_1\Gamma_2\mathbf{k}} \hat{B}_{\Gamma_1}^\dagger(\mathbf{k})T_{\Gamma_1\Gamma_2}(\mathbf{k})\hat{B}_{\Gamma_2}(\mathbf{k}) \quad (5)$$

in \mathbf{k} representation. Here the $\Gamma_{1,2}$ indices label different S or P excitons.

The $T(\mathbf{k})$ matrix for an isolated quartet of $S_{x,y}$ and $P_{x,y}$ excitons in 2D cuprates can be written as^{36,37}

$$T(\mathbf{k}) = \begin{pmatrix} E_S + 2T_S^\parallel \cos k_x & -2iT_{SP}^\parallel \sin k_x & T_S^\perp(1 + a(k_x, k_y)) & T_{SP}^\perp(1 + b(k_x, k_y)) \\ 2iT_{SP}^\parallel \sin k_x & E_P + 2T_P^\parallel \cos k_x & T_{SP}^\perp(1 - b(k_x, k_y)) & T_P^\perp(1 - a(k_x, k_y)) \\ T_S^\perp(1 + a^*(k_x, k_y)) & T_{SP}^\perp(1 - b^*(k_x, k_y)) & E_S + 2T_S^\parallel \cos k_y & -2iT_{SP}^\parallel \sin k_y \\ T_{SP}^\perp(1 + b^*(k_x, k_y)) & T_P^\perp(1 - a^*(k_x, k_y)) & 2iT_{SP}^\parallel \sin k_y & E_P + 2T_P^\parallel \cos k_y \end{pmatrix}, \quad (6)$$

where $a(k_x, k_y) = e^{ik_x} + e^{-ik_y}$, $b(k_x, k_y) = e^{ik_x} - e^{-ik_y}$. Two diagonal 2×2 blocks in this matrix are related to S_x, P_x and S_y, P_y excitons, respectively; off-diagonal blocks describe its coupling. Here a set of transfer parameters are introduced to describe the exciton dynamics

$$T_S^\parallel \approx -T_P^\parallel \approx \frac{1}{2}(t_e^{(3)} + t_h^{(3)}); \quad T_{SP}^\parallel \approx \frac{1}{2}(t_e^{(3)} - t_h^{(3)})$$

for the collinear exciton motion and

$$T_S^\perp \approx -T_P^\perp \approx \frac{1}{2}(t_e^{(2)} + t_h^{(2)}); \quad T_{SP}^\perp \approx \frac{1}{2}(t_e^{(2)} - t_h^{(2)})$$

for the 90° rotation of the exciton. The 90° rotation, or a “crab-like” motion, and 180° , or collinear motion of the exciton, are governed by the one-particle electron/hole transfer integrals $t_{e,h}^{(2,3)}$ for the next-nearest (nnn) and next-next-nearest ($nnnn$) CuO_4 centers, respectively. Hereafter we neglect higher-order terms which seem to be less important.

All these parameters have a rather clear physical sense. The electron (hole) transfer integrals $t_{e,h}^{(3)}$ for collinear exciton transfer ($R_{nnn} \approx 8\text{\AA}$) are believed to be smaller than $t_{e,h}^{(2)}$ integrals for rectangular transfer ($R_{nnn} \approx 4\sqrt{2}\text{\AA}$). In other words, the two-center excitons prefer to move crablike, rather than in the usual collinear mode. This implies a large difference for the excitonic dispersion in the $(0,0)$ - $(0,\pi)$ and

$(0,0)$ - (π,π) directions. The electronic wave function in the exciton (contrary to the hole one) has a dominant Cu $3d$ nature that implies a smaller value of the $t_e^{(2,3)}$ parameters compared with the $t_h^{(2,3)}$ ones.

It is worth noting that in Γ point $(0,0)$ the excitons form four modes of the A_{1g}, B_{1g} , and E_u symmetry. Figure 3 presents an example of the calculated excitonic dispersion along the nodal $(0,0)$ - (π,π) directions given reasonable values of different parameters: $(E_S - E_P) = 2|t_B| = 0.2$ eV; $T_S^\perp = -T_P^\perp = T_{SP}^\perp = 0.1$ eV, $T_S^\parallel = T_P^\parallel = T_{SP}^\parallel = 0$. In other words, we assume a nearest-neighbor approximation for the exciton transfer and neglect the electron transfer integrals as compared with the hole ones.

V. ANOTHER EXPERIMENTAL SIGNATURES OF THE ANOMALOUSLY SMALL TRUE CT GAP IN PARENT CUPRATES

Despite a successful explanation of the MIR absorption band features the main conjecture needs further independent experimental validation. First, it is worthwhile to notice one remarkable optical feature which was overlooked in earlier measurements. A weak but well-defined peak at $E_0 = 1570 \text{ cm}^{-1}$ (195 meV) in the optical conductivity has

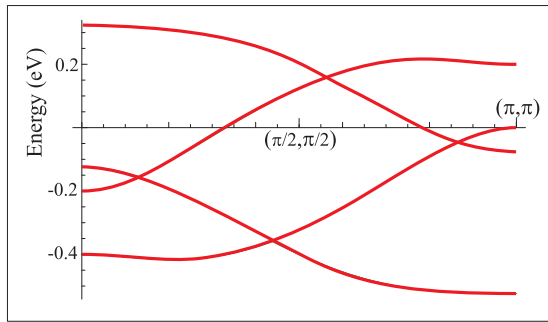


FIG. 3. (Color online) Dispersion of four EH dimer modes in the nodal $(0,0)$ - (π,π) direction.

been observed recently in $\text{Sr}_2\text{CuO}_2\text{Cl}_2$.¹⁹ The peak appears to strengthen and turn into a broadband with doping, whose peak softens rapidly. Such a behavior seems to be a typical one for the dipole-allowed S - P transition in the condensed EH dimers which transforms into a broad bosonic band with doping. It is worth noting that a similar peak at $E_0 \approx 1600 \text{ cm}^{-1}$ is clearly seen in the optical conductivity spectra of $\text{YBa}_2\text{Cu}_3\text{O}_6$.¹⁷ These experimental findings provide an unique opportunity to estimate the numerical value of the two-particle or local boson transfer integral t_B : $t_B \approx 0.1 \text{ eV}$, which is the value we have obtained from the nonlinear optical measurements.

A. Photoinduced absorption

Low-energy metastable EH dimers can be detected by photoinduced-absorption (PA) measurements. PA spectroscopy has become a very productive tool in the study both of the ground and excited electronic states. The energies and dynamics of the observed optical absorption are sensitive tools for determining the origins of the electronic energy gap within which these PAs are observed.

Two long-lived PA features peaking at 0.5 and 1.4 eV are observed in La_2CuO_4 ³⁸ with a crossover to photoinduced bleaching above 2.0 eV (see Fig. 4). These data, together with observed luminescence at $\leq 2 \text{ eV}$, confirm the existence of long-lived stable excited electronic CT states in this system. The PA peak at 0.5 eV can be naturally related to a photodissociation of the EH dimers, while a high-energy PA peak at 1.4 eV can be related to a photorecombination of the EH dimers or an inverse CT transition with the EH-pair annihilation.

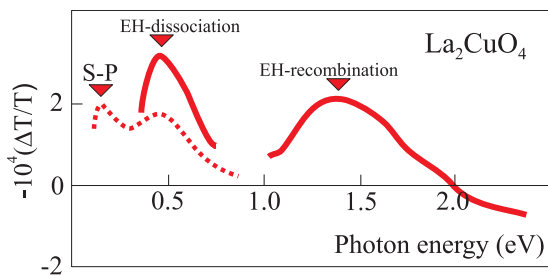


FIG. 4. (Color online) PA spectrum of La_2CuO_4 at 15 K taken with a pump photon energy of 2.54 eV.³⁸ Dotted curve presents the PA spectrum of La_2CuO_4 (arb. units) at 4.2 K taken with a pump photon energy of 2.7 eV.³⁹

A little bit later the photoexcitation measurements for La_2CuO_4 and Nd_2CuO_4 by Kim *et al.*³⁹ revealed a more intricate structure of the low-energy PA band with two peaks at 0.12 and 0.47 eV in La_2CuO_4 (see Fig. 4) and 0.16 and 0.62 eV in Nd_2CuO_4 with additional bleaching of the in-plane phonon-breathing modes. These low-energy peaks should be unambiguously attributed to S - P transitions in photogenerated EH dimers. PA features peaking near 1.5 eV with a crossover to photoinduced bleaching near 2.0 eV have been observed also in insulating Nd_2CuO_4 and $\text{YBa}_2\text{Cu}_3\text{O}_{6.2}$.⁴⁰ Similar effects have recently been observed in $\text{Sr}_2\text{CuO}_2\text{Cl}_2$.⁴¹ All of these strongly support the scenario and energy scheme in Fig. 1.

B. Raman scattering spectroscopy

The existence of low-energy CT excitations explains long-standing troubles in the Raman scattering spectra of parent insulating and doped cuprates. Usually the Raman scattering process is described by an effective Fleury–Loudon–Elliott spin Hamiltonian,⁴² which assumes that both initial and final states lie well below the CT gap. However, as for the LS theory of MIR absorption, the spin-only theory of Raman scattering runs into several difficulties. It cannot explain the large width with a clear asymmetry extending toward high energies.⁴² The most notable discrepancy with the Fleury–Loudon–Elliott theory is that, in addition to theoretically predicted B_{1g} excitation in the experiments, there is a comparable scattering intensity in A_{1g} polarizations and even in A_{2g} and B_{2g} polarizations of incident and outgoing light.⁴² However, an additional source for high-energy spectral features with the enhanced spectral weight and a complete collection of symmetries naturally arise from the coupling to the charge degrees of freedom. Indeed, at variance with the only B_{1g} spin excitation scenario here implies the existence of a whole collection of CT excitations (EH dimers) in the spectral range under consideration, with the E_u , A_{2g} symmetry for the p - d CT transitions and E_u , A_{1g} , B_{1g} symmetry for the d - d CT transitions, embracing both electric-dipole-allowed and forbidden electronic excitations displaying themselves in MIR absorption and Raman scattering, respectively.

Direct observation of the low-energy d - d CT transitions in $\text{Sr}_2\text{CuO}_2\text{Cl}_2$ has been performed in Ref. 43 using symmetry-selective resonant soft-x-ray Raman scattering (RSXRS) experiments at the O $1s$ edge excitation. Taking advantage of extremely weak elastic scattering intensity on the O $1s$ edge, the authors could observe both the generic 2-eV feature and a weak RSXRS structure around 0.5 eV in the controversial MIR region. The same photon polarization properties for both bands point to their common nature. In my opinion these are the FC and NFC d - d CT bands, respectively. (The 2M excitation can in principle also be observed at the oxygen K edge ($1s \rightarrow 2p$ transition).) Although the cross section for the oxygen K edge is relatively small, this case is interesting because the single-magnon excitation is forbidden here: There is no spin-orbit coupling for $1s$ core orbitals. Dispersive $\Delta S = 0$ excitations have been observed in La_2CuO_4 at both the Cu K and L edges.^{44,45} Figure 5 shows a possible RSXRS mechanism. The system begins in the GS, with nearest-neighbor $3d^9$ spins antiferromagnetically coupled. A $1s$ core-level electron is then

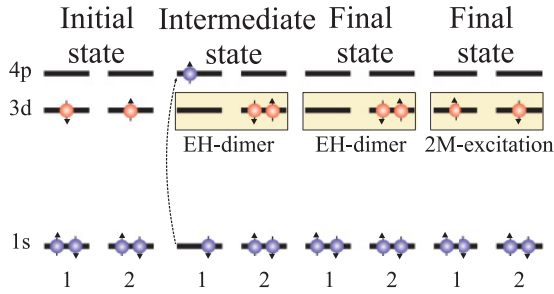


FIG. 5. (Color online) Possible resonant scattering process resulting in the creation of the EH dimer or the 2M excitation. The Cu (hole) spin on site 1 is repelled onto a neighboring site, site 2, by the $1s$ core hole in the intermediate state. Following the decay of the core hole, the wrong spin can hop back, resulting in spin flips on both sites.

excited into the $4p$ band. The resonance utilized in these experiments is that of the “well-screened” intermediate state, in which charge has moved in to screen the core hole from the oxygen ligand state. Further, it is energetically favorable for this hole to form a Zhang–Rice singlet on the neighboring sites thus creating an EH–dimer. When the $4p$ decays, the “wrong” spin hole can hop back with the net effect of the flipping of the two spins.

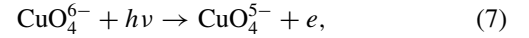
C. Photoemission spectroscopy

Angle-resolved photoemission spectroscopy (ARPES) is addressed to be a key experiment to elucidate a number of the principal issues of electronic theory related to the unconventional properties of cuprates.⁴⁶ Theoretically, ARPES measures the energy of an outgoing photoelectron with a known energy and momentum with respect to the chemical potential’s energy position. One supposes that ARPES can reconstruct the electronic band spectrum of a system in the whole Brillouin zone. However, the nature of the photoemission process itself, or in other words, the way the incident photon couples with the electronic states of the system in generating the photoemitted electrons is not yet understood. Even after years of intense ARPES studies for cuprates, there is still no full understanding of the renormalization effects and of the relevant energy scales in their electronic excitation spectrum.

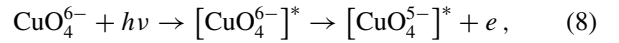
ARPES is the fast technique that implies an engagement of strong electron-lattice polarization effects that give rise to a specific shape of the photoemission spectra which reflects intensive FC transitions as well as weak NFC transitions. The whole spectral weight associated with a certain electron-removal state for the CT unstable parent cuprates will be spread over energies as large as several electron volts with a significant structure in momentum space. Obviously, these effects can hardly be caught by the simple t-J-Holstein model, where a photohole interacts with dispersionless optical phonons with the energies <0.1 eV through on-site local coupling.⁴⁷ Experimentally, usually one presents an ARPES study of the low-binding-energy occupied electronic structure, which corresponds to an investigation of the low-energy states. It is worth noting that *the true first electron-removal state certainly corresponds to the relaxed state; hence its ARPES portrait is*

formed by weak NFC transitions. Such a situation makes the analysis of ARPES spectra extremely ambiguous.

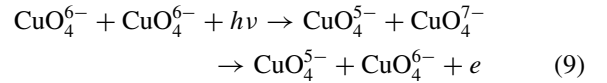
The photoemission process for a parent insulating cuprate implies overcoming the true CT gap. In other words, one way or another, the photoemission process



with the creation of a free electron should start with the excitation of the bound EH pair, and the photohole is born due to a reaction



or



for one- and two-center EH pairs, respectively. Here, $[\text{CuO}_4^{6-}]^*$ denotes a p - d CT state of the CuO_4^{6-} center, while $[\text{CuO}_4^{5-}]^*$ corresponds to a hole center in the low-energy non-Zhang–Rice states with the nominal $3d^{10}$ configuration on the Cu site. Indeed, the broadband at the binding energy ≤ 0.5 eV universally observed for parent cuprates both for nodal $(0,0)$ - (π,π) and antinodal $(0,0)$ - $(0,\pi)$ directions⁴⁶ can be related to the photoexcitation of the bound EH pair or EH dimer. Such a band in the vicinity of the antinodal “patches” most likely has nothing to do with any quasiparticle band features such as van Hove singularity.¹⁰ A noticeable dispersion of the 0.5-eV band can be attributed to the *EH-dimer dispersion rather than to any quasiparticle dispersion*. As was shown by Wang *et al.*, the singlet two-center CT exciton can move through the antiferromagnetic lattice rather freely, in contrast to the single-hole motion.

Angle-resolved electron energy-loss spectroscopy (EELS) measurements for $\text{Sr}_2\text{CuO}_2\text{Cl}_2$ ⁴⁸ point to a noticeable dispersion of the order of 0.2–0.3 eV for the optically excited d - d CT exciton that agrees with the experimentally observed dispersion for the “0.5-eV” band in ARPES spectra for this and other parent cuprates.⁴⁶ It is worth noting that a particularly striking dispersion ~ 0.3 eV of the d - d CT exciton has been revealed by angle-resolved EELS for the 1D cuprate Sr_2CuO_3 .²² Obviously, we should account for different selection rules and matrix element effects for EELS and ARPES.

The relationship between ARPES intensities and the underlying electronic structure can be quite complicated due to matrix element effects (see, e.g. Ref. 49), and caution should be exercised in interpreting detailed features of the ARPES intensities in terms of the spectral function. Nevertheless, the polarization-dependent ARPES measurements provide a sensitive test of the symmetries of the excitations with low binding energy.

VI. EVOLUTION OF CUPRATES WITH NONISOVALENT SUBSTITUTION

In contrast to a BaBiO_3 system, where we deal with a spontaneous generation of self-trapped CT excitons in the GS, the parent insulating cuprates are believed to be near excitonic instability when the self-trapped CT excitons form

the candidate relaxed excited states to struggle with the conventional GS.⁵⁰ In other words, the lattice relaxed CT excited state should be treated on an equal footing with the GS. Hence, cuprates are believed to be unconventional systems which are unstable, with regard to a self-trapping of the low-energy CT excitons with nucleation of EH droplets being actually the system of coupled electron CuO_4^{7-} and hole CuO_4^{5-} centers having been glued in the lattice due to strong electron-lattice polarization effects.

What is the evolution of the CuO_2 planes in the CT unstable cuprates under a nonisovalent doping? To describe the evolution we start with a very simple model⁵¹ which implies a quantum charge degree of freedom to be the only essential for the cuprate physics. We assume only three actual charge states of the CuO_4 plaquette: a bare center $M^0 = \text{CuO}_4^{6-}$, a hole center $M^{+1} = \text{CuO}_4^{5-}$, and an electron center $M^{-1} = \text{CuO}_4^{7-}$, respectively, forming the charge (isospin) triplet. The system of such charge triplets can be described in the framework of $S = 1$ pseudospin formalism. To this end we associate three charge states of the M center with different valences M^0, M^\pm with three components of the $S = 1$ pseudospin (isospin) triplet with $M_S = 0, \pm 1$, respectively. A complete set of the nontrivial pseudospin operators would include three spin-linear (dipole) operators $\hat{S}_{1,2,3}$ and five independent spin-quadrupole operators $\{\hat{S}_i, \hat{S}_j\} - \frac{2}{3}\hat{S}^2\delta_{ij}$. Accordingly, to describe different types of pseudospin ordering in such a mixed-valence system, we have to introduce eight order parameters: two classical *diagonal* order parameters $\langle \hat{S}_z \rangle$ and $\langle \hat{S}_z^2 \rangle$, and six *off-diagonal* order parameters $\langle \hat{S}_\pm \rangle$, $\langle \hat{S}_\pm^2 \rangle$, and $\langle \hat{T}_\pm \rangle$, where $\hat{T}_\pm = (\hat{S}_z \hat{S}_\pm + \hat{S}_\pm \hat{S}_z)$. Diagonal order parameter $\langle \hat{S}_z \rangle$ is related to a valence, or charge density with the electroneutrality constraint $\sum_i \langle \hat{S}_{iz} \rangle = \sum_i n_i = n$, while $\langle \hat{S}_z^2 \rangle = n_p$ determines the density of polar centers M^\pm , or “ionicity”. The *off-diagonal* order parameters describe different types of the valence mixing; in other words, these can change *valence* and *ionicity* with a specific phase ordering for the disproportionation reaction, single-particle transfer, and the two-particle transfer.

An effective pseudospin Hamiltonian of the model mixed-valence system can be written as

$$\begin{aligned} \hat{H} = & \sum_i (\Delta_i \hat{S}_{iz}^2 - h_i \hat{S}_{iz}) + \sum_{(i,j)} V_{ij} \hat{S}_{iz} \hat{S}_{jz} \\ & + \sum_{(i,j)} [D_{ij}^{(1)} (\hat{S}_{i+} \hat{S}_{j-} + \hat{S}_{i-} \hat{S}_{j+}) + D_{ij}^{(2)} \\ & \times (\hat{T}_{i+} \hat{T}_{j-} + \hat{T}_{i-} \hat{T}_{j+})] \\ & + \sum_{(i,j)} t_{ij} (\hat{S}_{i+}^2 \hat{S}_{j-}^2 + \hat{S}_{i-}^2 \hat{S}_{j+}^2). \end{aligned} \quad (10)$$

The two first single-ion terms describe the effects of a bare pseudospin splitting or the local energy of $M^{0,\pm}$ centers. The second term may be associated with a pseudomagnetic field h_i , in particular, a real electric field. It is easy to see that it describes an EH asymmetry. The third term describes the effects of short- and long-range interionic interactions, including screened Coulomb and covalent coupling. The last three terms in Eq. (10) representing the one- and two-particle hopping, are of primary importance for the transport properties, and

deserve special interest. Two types of one-particle hopping are governed by two transfer integrals $D^{(1,2)}$. The transfer integral $t'_{ij} = (D_{ij}^{(1)} + D_{ij}^{(2)})$ specifies the probability amplitude for a *local disproportionation*, or the *EH-pair creation*; $M^0 + M^0 \rightarrow M^\pm + M^\mp$; and the inverse process of the *EH-pair recombination*, $M^\pm + M^\mp \rightarrow M^0 + M^0$, while the transfer integral $t''_{ij} = (D_{ij}^{(1)} - D_{ij}^{(2)})$ specifies the probability amplitude for a polar center transfer, $M^\pm + M^0 \rightarrow M^0 + M^\pm$, or the *motion of the electron (hole) center in the matrix of M^0 centers* or motion of the M^0 center in the matrix of M^\pm centers. It should be noted that, if $t''_{ij} = 0$ but $t'_{ij} \neq 0$, the EH pair is locked in a two-site configuration. At variance with simple Hubbard-like models where all the types of one-electron (hole) transport are governed by the same transfer integral: $t'_{ij} = t''_{ij} = t_{ij}$, we deal with a “correlated” single-particle transport. The two-electron (hole) hopping is governed by a transfer integral t_{ij} , or a probability amplitude for the exchange reaction, $M^\pm + M^\mp \rightarrow M^\mp + M^\pm$, or the *motion of the electron (hole) center in the matrix formed by hole (electron) centers*. Obviously, both the \hat{S}_\pm and \hat{T}_\pm operators are fermionic, while \hat{S}_\pm^2 is a bosonic operator.

Simple uniform mean-field phases of the mixed-valence system include an insulating monovalent M^0 phase (parent cuprate), mixed-valence binary (disproportionated) M^\pm phase, and mixed-valence ternary (“under-disproportionated”) $M^{0,\pm}$ phase.⁵¹

In doped cuprates we deal with the EH injection to the insulating parent phase due to a nonisovalent substitution as in $\text{La}_{2-x}\text{Sr}_x\text{CuO}_4$, $\text{Nd}_{2-x}\text{Ce}_x\text{CuO}_4$, or change in oxygen stoichiometry as in $\text{YBa}_2\text{Cu}_3\text{O}_{6+x}$ and $\text{La}_2\text{CuO}_{4+\delta}$. Doping is not only to add charge carriers to the system but also to further reduce the gap between electron and hole bands in both electron- and hole-doped copper oxides.^{10,12,14} Anyway, the nonisovalent substitution produces natural centers for the condensation of the CT excitons and the *inhomogeneous nucleation* of EH droplets. Indeed, the gap Δ_{CT} for the thermal activation of uncoupled electron and hole centers shows a sudden drop from 0.89 to 0.53 eV upon doping of only 1% of the holes to the parent insulator La_2CuO_4 ¹² (or even to 0.25 eV¹⁰).

It means that nonisovalent substitution forms the impurity potential centers with a strong inhomogeneous electric field and reduced or even sign-reversed Δ_i values. At the very beginning of the nucleation regime in the heavily underdoped cuprates, the EH droplet nucleates as a nanoscopic cluster composed of several number of neighboring electron and hole centers pinned by disorder potential. As one of the remarkable experimental indications of the formation of the EH droplets, notice the zero-field copper NMR data in $\text{Y}_{1-x}\text{Ca}_x\text{Ba}_2\text{Cu}_3\text{O}_6$.⁵² The nonisovalent substitution in the antiferromagnetic state was accompanied by the anomalous decrease in the concentration of the NMR resonating copper nuclei. Every Ca^{2+} ion leaves out about 50 copper ions from the NMR, that could be related to their disproportionation within the EH droplet.

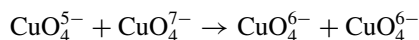
Hence, the nonisovalent substitution shifts the phase equilibrium from the parent insulating state (M^0 phase) to the binary disproportionated M^\pm phase, or a system of electron CuO_4^{7-} and hole CuO_4^{5-} centers. The system of strongly

correlated electron and hole centers appears to be equivalent to an unconventional EH Bose liquid (EHBL) in contrast with the EH Fermi liquid in conventional semiconductors. A simple model description of such a liquid implies a system of local singlet (S) bosons with a charge of $q = 2e$ moving in a lattice formed by hole centers. In a sense the local boson in this scenario represents an electronic equivalent of a Zhang–Rice singlet or the two-electron configuration $b_{1g}^2 A_{1g}$.

The doping in cuprates such as $\text{La}_{2-x}\text{Sr}_x\text{CuO}_4$ and $\text{Nd}_{2-x}\text{Ce}_x\text{CuO}_4$ gradually shifts the EHBL state away from half-filling, making the concentration of the local S bosons $n_B = 0.5 - x/2$ (LSCO) or $n_B = 0.5 + x/2$ (NCCO). Nonetheless, in both hole- and electron-doped cuprates we deal with S bosons moving on the lattice of the hole centers CuO_4^{5-} , that makes the unconventional properties of the hole centers common ones for both types of cuprates. It is clear that the EHBL scenario makes the doped cuprates the objects of *bosonic* physics. There is numerous experimental evidence that supports the bosonic scenario for doped cuprates.⁵³ In this connection, I would like to draw attention to the little-known results of comparative high-temperature studies of thermoelectric power and conductivity which unambiguously revealed the charge carriers with $q = 2e$, or two-electron (hole) transport.⁵⁴ The well-known relation $\frac{\partial \alpha}{\partial \ln \sigma} = \text{const} = -\frac{k}{q}$, with $|q| = 2|e|$, is fulfilled with high accuracy in the limit of high temperatures ($\sim 700\text{--}1000$ K) for different cuprates [$\text{YBa}_2\text{Cu}_3\text{O}_{6+x}$, $\text{La}_3\text{Ba}_3\text{Cu}_6\text{O}_{14+x}$, $(\text{Nd}_{2/3}\text{Ce}_{1/3})_4(\text{Ba}_{2/3}\text{Nd}_{1/3})_4\text{Cu}_6\text{O}_{16+x}$].

The evolution of the EH system under doping is particularly revealed in the infrared response of doped cuprates. The ab plane optical conductivity of 11 single crystals, belonging to the families $\text{Sr}_{2-x}\text{CuO}_2\text{Cl}_2$, $\text{Y}_{1-x}\text{Ca}_x\text{Ba}_2\text{Cu}_3\text{O}_6$, and $\text{Bi}_2\text{Sr}_{2-x}\text{La}_x\text{CuO}_6$, has been measured recently for a wide range of hole concentrations, $0 < p < 0.18$.¹⁹ At extreme dilution ($p = 0.005$), a weak narrow peak is first observed at ≈ 0.2 eV (see also Fig. 2) that we assign to a dipole-allowed S – P transition in isolated EH dimers at the energy $\approx 2|t_B|$. For increasing doping, that peak broadens into a far-infrared (FIR) band whose peak at ω_{FIR} softens rapidly with doping and whose low-energy edge sets the insulating gap for the bosonic system developed under doping. The insulator-to-metal transition (IMT) occurs when the softening of the FIR band closes the gap, thus evolving into a Drude term. In other words, the IMT in cuprates is driven by a conventional transformation of isolated EH-dimer levels into a conduction bosonic band at a critical p_{IMT} . As the Drude intensity progressively increases with doping the MIR band is no more resolved, though an additional oscillator in the MIR is required by all Drude–Lorentz fits to the spectra.⁵⁵

The EH dimer, or coupled EH pair, can be viewed as a negative- U center, where U , or the recombination energy (the energy of the inverse disproportionation reaction), defines an energy scale of a robustness of the EHBL phase. The corresponding intersite d – d CT recombination transition,



can be the first candidate for the most effective optical destruction of the EHBL, in particular, suppression of the boson condensate density (“Cooper pair-breaking” or CPB optical effect^{56,57}). It seems likely that the famous 1.5-eV peak

in the optical spectrum of a superconducting 123 system that reveals a fairly sharp CPB resonance⁵⁷ can be assigned to a an EH recombination transition with minimal energy. The rather large energy of such an exciton determines the stability of the EHBL phase with regard to its transformation to the bare parent insulating phase.

The minimal model of the EHBL is described by a Hamiltonian of local hardcore (hc) bosons on a lattice, which can be written in a standard form as follows:⁵⁸

$$H_{\text{hc}} = - \sum_{i>j} t_{ij} \hat{P} (\hat{B}_i^\dagger \hat{B}_j + \hat{B}_j^\dagger \hat{B}_i) \hat{P} + \sum_{i>j} V_{ij} N_i N_j - \mu \sum_i N_i, \quad (11)$$

where \hat{P} is the projection operator which removes double occupancy of any site. Here \hat{B}_i^\dagger (\hat{B}_i) are the Pauli creation (annihilation) operators, which are Bose-like, commuting for different sites $[\hat{B}_i, \hat{B}_j^\dagger] = 0$, if $i \neq j$, $[\hat{B}_i, \hat{B}_i^\dagger] = 1 - 2N_i$, $N_i = \hat{B}_i^\dagger \hat{B}_i$; N is a full number of sites; μ is the chemical potential determined from the condition of a fixed full number of bosons $N_i = \sum_{i=1}^N \langle N_i \rangle$ or concentration $n = N_i/N \in [0, 1]$. The t_{ij} denotes an effective transfer integral, and V_{ij} is an intersite interaction between the bosons. It is worth noting that near half-filling ($n \approx 1/2$) one might introduce the renormalization $N_i \rightarrow (N_i - 1/2)$, or neutralizing background that immediately provides the particle-hole symmetry.

The model of hardcore bosons with an intersite repulsion is equivalent to a system of spins $s = 1/2$ exposed to an external magnetic field in the z direction. For the system with neutralizing background we arrive at an effective pseudospin Hamiltonian,

$$H_{\text{hc}} = \sum_{i>j} J_{ij}^{xy} (\hat{s}_i^+ \hat{s}_j^- + \hat{s}_j^+ \hat{s}_i^-) + \sum_{i>j} J_{ij}^z \hat{s}_i^z \hat{s}_j^z - \mu \sum_i \hat{s}_i^z, \quad (12)$$

where $J_{ij}^{xy} = 2t_{ij}$, $J_{ij}^z = V_{ij}$, $\hat{s}^- = \frac{1}{\sqrt{2}} \hat{B}$, $\hat{s}^+ = -\frac{1}{\sqrt{2}} \hat{B}^\dagger$, $\hat{s}^z = -\frac{1}{2} + \hat{B}_i^\dagger \hat{B}_i$, $\hat{s}^\pm = \mp \frac{1}{\sqrt{2}} (\hat{s}^x \pm i \hat{s}^y)$.

The model of quantum lattice Bose gas has a long history and has been suggested initially for conventional superconductors⁵⁹ and quantum crystals such as ^4He where superfluidity coexists with a crystalline order.^{60,61} Subsequently, the Bose-Hubbard (BH) model was studied as a model of the superconductor-insulator transition in materials with local bosons, bipolarons, or preformed Cooper pairs.^{62,63} 2D BH models have been addressed as relevant to describe the superconducting films and Josephson junction arrays. The most recent interest in the system of hardcore bosons comes from the delightful results on Bose–Einstein (BE) condensed atomic systems produced by trapping bosonic neutral atoms in an optical lattice.⁶⁴

One of the fundamental hot debated problems in bosonic physics concerns the evolution of the charge-ordered (CO) GS of 2D hardcore bosons with a doping away from half-filling. Numerous model studies steadily confirmed the emergence of “supersolid” CO + BS phases with simultaneous diagonal CO and off-diagonal BS long-range order. Quantum Monte Carlo (QMC) simulations⁶⁵ found two significant features of the 2D hard boson model with a screened Coulomb

repulsion: the absence of a supersolid phase at half-filling and a growing tendency to phase separation (CO + BS) upon doping away from half-filling. Moreover, Batrouni and Scalettar⁶⁵ studied quantum phase transitions in the GS of the 2D hardcore boson Hamiltonian and showed numerically that, contrary to the generally held belief, the most commonly discussed “checkerboard” supersolid is thermodynamically unstable and the phase separates into solid and superfluid phases. The physics of the CO + BS phase separation in the BH model is associated with a rapid increase of the energy of a homogeneous CO state with doping away from half-filling due to a large “pseudospin-flip” energy cost. Hence, it appears to be energetically more favorable to “extract” extra bosons (holes) from the CO state and arrange them into finite clusters with a relatively small number of particles. Such a droplet scenario is believed to minimize the long-range Coulomb repulsion.

The EHBL in cuprates evolves from the parent phase through to the nucleation of nanoscopic EH droplets around self-trapped CT excitons. However, the EHBL itself is unstable with regard to a so-called topological phase separation.⁵⁸ For instance, deviation from half-filling in EHBL of quasi-2D cuprates is accompanied by the formation of a multicenter topological defect such as CO bubble domain(s) with BS and extra bosons both localized in domain wall(s), or a topological CO + BS phase separation, rather than a uniform mixed CO + BS supersolid phase. A nanosize model of the simplest topological defect is suggested in Ref. 58. Symmetry of the order parameter distribution in the domain wall appears to be specified only by the sign of the boson transfer integral. The problem of the order parameter associated with the bubble domain is much more complicated than in the conventional BCS-like approach due to its multicomponent nature. It is worth noting that, in the framework of a BCS-like scenario, the symmetry of the order parameter is strictly defined in a momentum space albeit the discussion of different experimental data has usually been performed with a real-space distributed order parameter. In fact, the EHBL represents a system with different symmetry of low-lying excited states and competing order parameters that implies their possible ambiguous manifestation in either properties. The relative magnitude and symmetry of multicomponent order parameters are mainly determined by the sign of the nn and nnn bosonic transfer integrals. In general, the topologically inhomogeneous phase of the hc boson system away from the half-filling can exhibit the signatures of s , d , and even p symmetry of the off-diagonal order. Indeed, numerous experimental findings point to a more intricate picture with the symmetry of the superconducting state than is claimed in the conventional uniform d -wave superconductivity.

The long-wavelength behavior of the hc boson system is believed to reveal many properties typical for granular superconductors, charge density wave materials, Wigner crystals, and a multiskyrmion system akin to a quantum Hall ferromagnetic state of a 2D electron gas.^{66,67} With decreasing the temperature we deal with an isotropic liquid phase, liquid crystal, and crystallization of the multiskyrmion system, respectively; namely these charged topological defects with a concentration proportional to the hole-/electron doping x , rather than single local bosons, can be effective charge carriers in doped cuprates.

Making use of a QMC technique we have studied the evolution of the phase state of CuO₂ planes in a model CT unstable cuprate La_{2-x}Sr_xCuO₄.⁶⁸ Tentative results show that the nonisovalent doping gives rise to a nucleation of the inhomogeneous supersolid CO + BS phase characterized by charge and off-diagonal BS order parameters whose competition results in a generic T - x phase diagram where a pseudogap temperature $T^*(x)$ points to an onset of the CO ordering and a temperature $T_v(x) > T_c(x)$ with a domelike x dependence points to an onset of the long-lived BS fluctuations with all the signatures of a local superconductivity. The transition to a bulk 3D coherent superconducting state corresponds to the percolation threshold among the locally superconducting regions.

It should be emphasized that the minimal model of the EHBL phase in cuprates does not imply intervention of orbital and spin degrees of freedom. Indeed, the model considers a system of the spin and orbital singlet $^1A_{1g}$ local S bosons moving on the lattice formed by hole centers with the well isolated spin and orbital singlet Zhang–Rice $^1A_{1g}$ GS.

However, both theoretical considerations and experimental data point toward a more complicated nature of the valence hole states in doped cuprates than predicted by the simple Zhang–Rice model. Actually, we deal with a competition of conventional hybrid Cu 3d–O 2p $b_{1g} \propto d_{x^2-y^2}$ state and a pure oxygen nonbonding state with a_{2g} and $e_{ux,y} \propto p_{x,y}$ symmetry.^{69,70} Accordingly, the GS of such a non-Zhang–Rice hole center CuO₄⁵⁻ as a cluster analog of Cu³⁺ ion should be described by a complex $^1A_{1g}^{-1,3}B_{2g}^{-1,3}E_u$ multiplet with several competing charge, orbital, and spin order parameters, both conventional ones (e.g., spin moment or Ising-like orbital magnetic moment) and unconventional, or hidden, ones (e.g., intraplaquette’s staggered order of Ising-like oxygen orbital magnetic moment or combined spin-quadrupole ordering). The non-Zhang-Rice hole CuO₄⁵⁻ centers should be considered as singlet-triplet pseudo-Jahn–Teller (ST-PJT) centers prone to a strong vibronic coupling. A novel state of cuprate matter is characterized by a multicomponent order parameter including charge density, $U(1)$ global phase, electric dipole and quadrupole moments, and a circular orbital current generated by oxygen holes.^{69,70} The non-Zhang–Rice structure of the hole CuO₄⁵⁻ centers forming a lattice for the local boson motion manifests itself in many unconventional properties of the doped cuprates, which are often addressed to be signatures of some mechanism of the HTSC.

Obviously, the local S bosons do interact with the lattice of the hole centers, both as a simple source of fluctuating electric fields and in a more complex way, in particular, due to a suppression of the ST-PJT order parameters on the hole center occupied by the S boson, that is on the electron center CuO₄⁷⁻, characterized by occupied Cu 3d¹⁰ and O 2p⁶ orbitals. The role of the ST-PJT or non-Zhang–Rice structure of hole centers in superconductivity seems to be merely negative due to effect of a vibronic reduction of the S boson transfer integral and according increase of its effective mass.⁷¹ At the same time, the lattice of the ST-PJT hole centers with its large polarizability does provide an effective screening of the boson-boson repulsion, thus promoting high T_c ’s. Anyway, the crucial role of electron-lattice polarization effects of the order

of 1 eV in HTSC should be emphasized; namely, these effects are believed to provide a glue to stabilize the EH structure of the EHBL phase.

VII. CONCLUSION

A large body of experimental data points toward a CT instability of parent insulating cuprates as being their unique property. It is argued that the true CT gap in these compounds is as small as 0.4–0.5 eV rather than 1.5–2.0 eV as usually derived from the optical gap measurements. In fact we deal with a competition of the conventional ($3d^9$) ground state and a CT state with the formation of EH dimers, which evolves under doping to an unconventional bosonic system. An attempt was made to incorporate a broad-enough collection of experimental results to demonstrate validity of the main message. The conjecture does provide unified standpoint on the main experimental findings for parent cuprates including linear and

nonlinear optical, Raman, photoemission, photoabsorption, and transport properties. The model approach suggested is believed to provide a conceptual framework for an in-depth understanding of physics of strongly correlated oxides such as cuprates, manganites, bismuthates, and other systems with CT excitonic instability and/or mixed valence. An attempt is not made here to provide any strict theoretical analysis. The facts that are pointed to are obtained from the unified analysis of optical, Raman, ARPES, XPS, and Hall experimental data.

In a sense, this paper provides a validation of a so-called “disproportionation” scenario in cuprates which was addressed earlier by many authors; however, up until now it was not properly developed.

ACKNOWLEDGMENT

RFBR Grant No. 10-02-96032 is acknowledged for financial support.

-
- ¹J. G. Bednorz and K. A. Müller, *Z. Phys. B* **4**, 189 (1986).
²A. S. Moskvin, *Physica B* **252**, 186 (1998); A. S. Moskvin and A. S. Ovchinnikov, *J. Magn. Magn. Mater.* **186**, 288 (1998); *Physica C* **296**, 250 (1998); A. S. Moskvin and Yu. D. Panov, *Phys. Status Solidi B* **212**, 141 (1999); *J. Phys. Chem. Solids* **60**, 607 (1999); A. S. Moskvin, in *Proceedings of the Second International Conference on Fundamental Problems of High-Temperature Superconductivity, 9–13 October (2006)* (Moscow-Zvenigorod, 2006), p. 73; A. S. Moskvin and Yu. D. Panov, in *Proceedings of the Third International Conference on Fundamental Problems of High-Temperature Superconductivity, 13–17 October (2008)* (Moscow-Zvenigorod, 2008), p. 56.
³J. E. Hirsch and D. J. Scalapino, *Phys. Rev. B* **32**, 5639 (1985); C. M. Varma, *Phys. Rev. Lett.* **61**, 2713 (1988); J. A. Wilson, *J. Phys. Condens. Matter* **12**, R517 (2000); T. H. Geballe and B. Y. Mozyshes, *Physica C* **341–348**, 1821 (2000); S. Larsson, *Int. J. Quantum Chem.* **90**, 1457 (2002); *Physica C* **460–462**, 1063 (2007); K. V. Mitsen and O. M. Ivanenko, *Phys. Usp.* **47**, 493 (2004); K. D. Tsendin, B. P. Popov, and D. V. Denisov, *Supercond. Sci. Technol.* **19**, 313 (2006); H. Katayama-Yoshida, K. Kusakabe, H. Kizaki, and A. Nakanishi, e-print [arXiv:0807.3770v1](https://arxiv.org/abs/0807.3770v1).
⁴T. Mizokawa, D. I. Khomskii, and G. A. Sawatzky, *Phys. Rev. B* **61**, 11263 (2000).
⁵A. S. Moskvin, T. Mizokawa, D. I. Khomskii, and G. A. Sawatzky, *Phys. Rev. B* **79**, 115102 (2009).
⁶R. Cabassi, F. Bolzoni, E. Gilioli, F. Bissoli, A. Prodi, and A. Gauzzi, *Phys. Rev. B* **81**, 214412 (2010).
⁷S. P. Ionov, G. V. Ionova, V. S. Lubimov, and E. F. Makarov, *Phys. Status Solidi B* **71**, 11 (1975).
⁸C. Franchini, G. Kresse, and R. Podloucky, *Phys. Rev. Lett.* **102**, 256402 (2009).
⁹J. B. Goodenough, *J. Supercond.* **13**, 793 (2000).
¹⁰L. P. Gorkov and G. B. Teitelbaum, *Phys. Rev. Lett.* **97**, 247003 (2006); *J. Phys. Conf. Ser.* **108**, 012009 (2008).
¹¹F. Carbone, N. Gedik, J. Lorenzana, and A. H. Zewail, *Adv. Condens. Matter Phys.* **2010**, 958618.
¹²Y. Ando, Y. Kurita, S. Komiya, S. Ono, and K. Segawa, *Phys. Rev. Lett.* **92**, 197001 (2004); S. Ono, S. Komiya, and Y. Ando, *Phys. Rev. B* **75**, 024515 (2007).
¹³M. Ikeda, M. Takizawa, T. Yoshida, A. Fujimori, K. Segawa, and Y. Ando, e-print [arXiv:1001.0102v1](https://arxiv.org/abs/1001.0102v1).
¹⁴T. Xiang, H. G. Luo, D. H. Lu, K. M. Shen, and Z. X. Shen, *Phys. Rev. B* **79**, 014524 (2009).
¹⁵M. A. Kastner, R. J. Birgeneau, G. Shirane, and Y. Endoh, *Rev. Mod. Phys.* **70**, 897 (1998); M. Grüninger, J. Münzel, A. Gaymann, A. Zibold, H. P. Geserich, and T. Kopp, *Europhys. Lett.* **35**, 55 (1996).
¹⁶J. D. Perkins, R. J. Birgeneau, J. M. Graybeal, M. A. Kastner, and D. S. Kleinberg, *Phys. Rev. B* **58**, 9390 (1998).
¹⁷M. Grüninger, D. van der Marel, A. Damascelli, A. Erb, T. Nunner, and T. Kopp, *Phys. Rev. B* **62**, 12422 (2000).
¹⁸S. L. Cooper, D. Reznik, A. Kotz, M. A. Karlow, R. Liu, M. V. Klein, W. C. Lee, J. Giapintzakis, D. M. Ginsberg, B. W. Veal, and A. P. Paulikas, *Phys. Rev. B* **47**, 8233 (1993).
¹⁹D. Nicoletti, P. Di Pietro, O. Limaj, P. Calvani, U. Schade, S. Ono, Y. Ando, and S. Lupi, e-print [arXiv:1101.0745v2](https://arxiv.org/abs/1101.0745v2).
²⁰J. Lorenzana and G. A. Sawatzky, *Phys. Rev. Lett.* **74**, 1867 (1995).
²¹A. S. Moskvin, R. Neudert, M. Knupfer, J. Fink, and R. Hayn, *Phys. Rev. B* **65**, 180512(R) (2002).
²²A. S. Moskvin, J. Málek, M. Knupfer, R. Neudert, J. Fink, R. Hayn, S.-L. Drechsler, N. Motoyama, H. Fisaki, and S. Uchida, *Phys. Rev. Lett.* **91**, 037001 (2003).
²³Ran Liu, D. Salamon, M. V. Klein, S. L. Cooper, W. C. Lee, S.-W. Cheong, and D. M. Ginsberg, *Phys. Rev. Lett.* **71**, 3709 (1993).
²⁴N. S. Headings, S. M. Hayden, R. Coldea, and T. G. Perring, *Phys. Rev. Lett.* **105**, 247001 (2010).
²⁵V. V. Struzhkin, A. F. Goncharov, H. K. Mao, R. J. Hemley, S. W. Moore, J. M. Graybeal, J. Sarrao, and Z. Fisk, *Phys. Rev. B* **62**, 3895 (2000).
²⁶S. V. Dordevic, L. W. Kohlman, L. C. Tung, Y.-J. Wang, A. Gozar, G. Logvenov, and I. Bozovic, *Phys. Rev. B* **79**, 134503 (2009).
²⁷F. C. Zhang and T. M. Rice, *Phys. Rev. B* **37**, 3759 (1988).

- ²⁸P. W. Anderson, *J. Phys. Chem. Solids* **59**, 1675 (1998).
- ²⁹T. Ogasawara, M. Ashida, N. Motoyama, H. Eisaki, S. Uchida, Y. Tokura, H. Ghosh, A. Shukla, S. Mazumdar, and M. Kuwata-Gonokami, *Phys. Rev. Lett.* **85**, 2204 (2000).
- ³⁰A. Schülzgen, Y. Kawabe, E. Hanamura, A. Yamanaka, P.-A. Blanche, J. Lee, H. Sato, M. Naito, N. T. Dan, S. Uchida, Y. Tanabe, and N. Peyghambarian, *Phys. Rev. Lett.* **86**, 3164 (2001).
- ³¹H. Kishida, H. Matsuzaki, H. Okamoto, T. Manabe, M. Yamashita, Y. Taguchi, and Y. Tokura, *Nature London* **405**, 929 (2000).
- ³²M. Ono, K. Miura, A. Maeda, H. Matsuzaki, H. Kishida, Y. Taguchi, Y. Tokura, M. Yamashita, and H. Okamoto, *Phys. Rev. B* **70**, 085101 (2004).
- ³³H. Kishida, M. Ono, K. Miura, H. Okamoto, M. Izumi, T. Manako, M. Kawasaki, Y. Taguchi, Y. Tokura, T. Tohyama, K. Tsutsui, and S. Maekawa, *Phys. Rev. Lett.* **87**, 177401 (2001).
- ³⁴A. Maeda, M. Ono, H. Kishida, T. Manako, A. Sawa, M. Kawasaki, Y. Tokura, and H. Okamoto, *Phys. Rev. B* **70**, 125117 (2004).
- ³⁵A. S. Davydov, *Theory of Molecular Excitons* (McGraw-Hill, New York, 1962).
- ³⁶Y. Y. Wang, F. C. Zhang, V. P. Dravid, K. K. Ng, M. V. Klein, S. E. Schnatterly, and L. L. Miller, *Phys. Rev. Lett.* **77**, 1809 (1996); F. C. Zhang and K. K. Ng, *Phys. Rev. B* **58**, 13520 (1998).
- ³⁷A. S. Moskvin, S.-L. Drechsler, R. Hayn, and J. Málek, e-print [arXiv:cond-mat/0507707](https://arxiv.org/abs/cond-mat/0507707) (unpublished).
- ³⁸J. M. Ginder, M. G. Roe, Y. Song, R. P. McCall, J. R. Gaines, E. Ehrenfreund, and A. J. Epstein, *Phys. Rev. B* **37**, 7506 (1988).
- ³⁹Y. H. Kim, S.-W. Cheong, and Z. Fisk, *Phys. Rev. Lett.* **67**, 2227 (1991).
- ⁴⁰K. Matsuda, I. Hirabayashi, K. Kawamoto, T. Nabatame, T. Tokizaki, and A. Nakamura, *Phys. Rev. B* **50**, 4097 (1994).
- ⁴¹J. S. Dodge, A. B. Schumacher, L. L. Miller, and D. S. Chemla, e-print [arXiv:0910.5048v1](https://arxiv.org/abs/0910.5048v1).
- ⁴²T. P. Devereaux and R. Hackl, *Rev. Mod. Phys.* **79**, 175 (2007).
- ⁴³Y. Harada, K. Okada, R. Eguchi, A. Kotani, H. Takagi, T. Takeuchi, and S. Shin, *Phys. Rev. B* **66**, 165104 (2002).
- ⁴⁴J. P. Hill, G. Blumberg, Y.-J. Kim, D. S. Ellis, S. Wakimoto, R. J. Birgeneau, S. Komiyama, Y. Ando, B. Liang, R. L. Greene, D. Casa, and T. Gog, *Phys. Rev. Lett.* **100**, 097001 (2008); D. S. Ellis, J. Kim, J. P. Hill, S. Wakimoto, R. J. Birgeneau, Y. Shvyd'ko, D. Casa, T. Gog, K. Ishii, K. Ikeuchi, A. Paramakanti, and Y.-J. Kim, *Phys. Rev. B* **81**, 085124 (2010).
- ⁴⁵L. Braicovich *et al.*, *Phys. Rev. Lett.* **102**, 167401 (2009).
- ⁴⁶A. Damascelli, Z. Hussain, and Z.-X. Shen, *Rev. Mod. Phys.* **75**, 473 (2003).
- ⁴⁷A. S. Mishchenko and N. Nagaosa, *Phys. Rev. Lett.* **93**, 36402 (2004).
- ⁴⁸R. Neudert *et al.*, *Physica B* **230–232**, 847 (1997); J. Fink *et al.*, *ibid.* **237–238**, 93 (1997).
- ⁴⁹A. S. Moskvin, E. N. Kondrashov, and V. I. Cherepanov, *Physica B* **311**, 200 (2002).
- ⁵⁰K. Nasu, ed., *Relaxations of Excited States and Photo Induced Structural Phase Transitions*, vol. 124 of Springer Series on Solid-State Sciences (Springer New York, 1997), p. 17.
- ⁵¹A. S. Moskvin, *Low Temp. Phys.* **33**, 234 (2007).
- ⁵²P. Mendels and H. Alloul, *Physica C: Superconductivity* **156**, 355 (1988).
- ⁵³A. S. Alexandrov and N. F. Mott, *J. Supercond.* **7**, 599 (1994); A. S. Alexandrov, *Physica C* **305**, 46 (1998).
- ⁵⁴I. A. Leonidov, Ya. N. Blinovskov, E. E. Flyatau, P. Ya. Novak, and V. L. Kozhevnikov, *Physica C* **158**, 287 (1989); M.-Y. Su, C. E. Elsbernd, and T. O. Mason, *J. Am. Ceram. Soc.* **73**, 415 (1990); E. B. Mitberg, M. V. Patrakeev, A. A. Lakhtin, I. A. Leonidov, V. L. Kozhevnikov, and K. R. Poepelmeier, *J. Alloys Compd.* **274**, 103 (1998).
- ⁵⁵The MIR absorption for the EHBL phase can be related to the dipole-allowed charge transfer p - d transition ${}^1A_{1g} \rightarrow {}^1E_u$ in hole CuO_4^{5-} centers (see Ref. 2)
- ⁵⁶Y. G. Zhao, Eric Li, Tom Wu, S. B. Ogale, R. P. Sharma, T. Venkatesan, J. J. Li, W. L. Cao, C. H. Lee, H. Sato, and M. Naito, *Phys. Rev. B* **63**, 132507 (2001).
- ⁵⁷E. Li, R. P. Sharma, S. B. Ogale, Y. G. Zhao, T. Venkatesan, J. J. Li, W. L. Cao, and C. H. Lee *Phys. Rev. B* **65**, 184519 (2002); E. Li, R. P. Sharma, S. B. Ogale, V. N. Krivoruchko, and R. V. Petryuk, *ibid.* **66**, 134520 (2002).
- ⁵⁸A. S. Moskvin, I. G. Bostrem, and A. S. Ovchinnikov, *JETP Lett.* **78**, 772 (2003); A. S. Moskvin, *Phys. Rev. B* **69**, 214505 (2004).
- ⁵⁹M. R. Schafroth, *Phys. Rev.* **100**, 463 (1955).
- ⁶⁰H. Matsuda and T. Tsuneto, *Suppl. Prog. Theor. Phys.* **46**, 411 (1970).
- ⁶¹K. Liu and M. Fisher, *J. Low Temp. Phys.* **10**, 655 (1973).
- ⁶²K. Kubo and S. Takada, *J. Phys. Soc. Jpn.* **52**, 2108 (1983).
- ⁶³R. Micnas, J. Ranninger, and S. Robaszkiewicz, *Rev. Mod. Phys.* **62**, 113 (1990).
- ⁶⁴M. Greiner, O. Mandel, T. Esslinger, T. W. Hänsch, and I. Bloch, *Nature London* **415**, 39 (2002).
- ⁶⁵G. G. Batrouni and R. T. Scalettar, *Phys. Rev. Lett.* **84**, 1599 (2000); F. Hébert, G. G. Batrouni, R. T. Scalettar, G. Schmid, M. Troyer, and A. Dorneich, *Phys. Rev. B* **65**, 014513 (2001); G. Schmid, S. Todo, M. Troyer, and A. Dorneich, *Phys. Rev. Lett.* **88**, 167208 (2002).
- ⁶⁶A. G. Green, *Phys. Rev. B* **61**, R16299 (2000).
- ⁶⁷C. Timm, S. M. Girvin, and H. A. Fertig, *Phys. Rev. B* **58**, 10634 (1998).
- ⁶⁸A. S. Moskvin and A. V. Korolev (unpublished).
- ⁶⁹A. S. Moskvin, *JETP Lett.* **80**, 697 (2004).
- ⁷⁰A. S. Moskvin and Yu. D. Panov, *Fiz. Nizk. Temp. [Low Temp. Phys.]* **37**, 334 (2011).
- ⁷¹A. S. Moskvin and Yu. D. Panov, *JETP* **84**, 354 (1997).